Effects of random fields on the phase diagram of $Mn_{0.875}Zn_{0.125}F_2$

Y. Shapira
Francis Bitter National Magnet Laboratory, Massachusetts Institute of Technology, Cambridge, Massachusetts 02139

N. F. Oliveira, Jr.
Instituto de Fisica, Universidade de São Paulo, Caixa Postale 20516, São Paulo, Brazil
(Received 25 October 1982)

Phase transitions in $Mn_{1-x}Zn_xF_2$, $x=0.125$, were investigated using thermal-expansion, magnetostriction, and ultrasonic-attenuation measurements. The phase diagram was determined for 4.2 K $\leq T \leq T_N$ and $0 \leq H \leq 140$ kOe, where $T_N = 58.4$ K is the Néel temperature. The magnetic field $\vec{H}$ was parallel to [001]. The random field H_R induced by H influences the shape of the λ anomaly at the paramagnetic-antiferromagnetic transition, and depresses the transition temperature $T_c^{\parallel}$. Some evidence for an irreversible behavior near $T_c^{\parallel}$ is found for $H \neq 0$. The paramagnetic–spin-flop boundary $T_c^{\perp}(H)$ exhibits a large "bulge" towards high T. At 4.2 K, the spin-flop field H_{sf} is 78 kOe, which is lower than that predicted by mean-field theory. The discrepancy is explained by considering the effect of the random fields. As T increases from 4.2 K, H_{sf} first increases but then decreases as T approaches the bicritical temperature $T_b = 55$ K. It is possible that the latter portion of the spin-flop line is actually one of two second-order lines which surround an intermediate phase. The Néel temperature is in reasonable agreement with mean-field theory.

I. INTRODUCTION

The dramatic influence of random quenched magnetic fields on critical behavior has been discussed theoretically for nearly a decade. The early work of Imry and Ma[1] showed that the upper critical dimension changes from 4 to 6 and that the lower critical dimension increases. Later works considered scaling laws,[2] critical exponents,[3] and phase diagrams[4] in the presence of random fields.

An important issue which is still being debated is the lower critical dimension d_l for the Ising model in a random field. An early domain-wall argument[1] suggested that $d_l = 2$ so that a long-range order can exist for the usual lattice dimensionality $d = 3$. However, in several of the recent theoretical papers (e.g., Refs. 5 and 6) it was concluded that $d_l = 3$ and that no long-range order can exist at finite temperatures T for $d = 3$. In this case, there is no genuine second-order transition for $d = 3$. An estimate for the smearing of the apparent transition was given.[6] In contrast to these results, a very recent theoretical work by Grinstein and Ma[7] gives $d_l = 2$.

A significant advance toward the experimental realization of random fields was made by Fishman and Aharony.[8] They showed that a random staggered magnetic field $\vec{H}_R$ is produced in an easy-axis antiferromagnet when (1) the exchange interactions are random, and (2) a magnetic field $\vec{H}$ is applied parallel to the easy axis. The situation is then similar to that of a uniaxial ferromagnet in a uniaxial random field. The random field in the antiferromagnet is proportional to the magnetization M which near the Néel temperature T_N is proportional to H. For a given M, H_R increases when the randomness in the exchange constants increases. For $H = 0$ there is no random field and the critical behavior is practically the same as that of the pure antiferromagnet, i.e., Ising-like. When $\vec{H}$ is applied, a crossover to a random-field Ising behavior takes place. The character of the transitions and the phase boundaries near the bicritical point were discussed by Bray.[9]

To produce random fields experimentally one usually uses a diluted antiferromagnet in which some of the magnetic ions were replaced by nonmagnetic "impurities." It is assumed (more correctly, hoped) that the impurities are randomly distributed. The system then corresponds to a random-site model rather than to the random-bond model of Fishman and Aharony. It has been recently shown that in the random-site case there is an additional contribution to H_R beyond that which exists in the random-bond case.[10] Another feature of a randomly diluted anti-

 ©1983 The American Physical Society

ferromagnet is the change in the local crystal symmetry.[11] We expect that this last complicating feature is not of major significance in the present work because Mn^{2+} is an S-state ion with a small spin-lattice coupling, and the dipole-dipole interaction is weak compared to the exchange interaction.

Only a few experimental investigations of random fields were performed until now. The bicritical region of La- and Bi-doped $GdA10_3$ was investigated by Rohrer *et al.*[12] Some, but not all, of the theoretical predictions were confirmed. The phase diagram of $Mn_{0.96}Zn_{0.04}F_2$ was measured in fields up to 175 kOe.[13] Again, some (but not all) of the theoretical predictions were confirmed. Transitions in more heavily doped samples of MnF_2 and FeF_2 were studied at relatively low H with the use of optical birefringence.[14] The specific heat of Mg-doped $FeCl_2$ was studied by Wong *et al.*[10] The last two studies confirmed the Fishman-Aharony prediction for the influence of H_R on the shape of the phase boundary at low H.[8] A neutron-diffraction study of two-dimensional and three-dimensional diluted antiferromagnets was performed by Yoshizawa *et al.*[15] The results were consistent with $d_l=3$.

In the present work the phase transitions of $Mn_{0.875}Zn_{0.125}F_2$ were studied in magnetic fields up to 140 kOe. Much of the terminology which will be used is borrowed from the phase diagram of a pure easy-axis antiferromagnet, such as MnF_2. The modern theory for this phase diagram is discussed in Refs. 16 and 17. When $\vec{H}$ is parallel to the easy axis there are three phases: the disordered paramagnetic (P) phase, the antiferromagnetic (AF) phase in which the staggered magnetization is parallel to the easy axis, and the spin-flop (SF) phase with a perpendicular staggered magnetization. There are two second-order phase boundaries: the P-AF line $T_c^{\parallel}(H)$ and P-SF line $T_c^{\perp}(H)$. In addition, a first-order boundary, $H_{sf}(T)$, separates the AF and SF phases. All three phase boundaries meet at the bicritical point (BCP). In the present case of Zn-doped MnF_2, the critical behavior on the line $T_c^{\parallel}(H)$ is expected to be affected by random fields (except at $H=0$). The transitions on this line are then genuine or not, depending on whether $d_l=2$ or 3. For convenience we shall use the words "transition" and "phase boundary" in reference to the line $T_c^{\parallel}(H)$ even though d_l might be equal to 3. In the random-bond model the critical behavior on the line $T_c^{\perp}$ (but not the shape of this line) is expected to be similar to that in the pure material.

In discussing our results we shall make comparisons with the phase diagram of pure MnF_2. For this tetragonal antiferromagnet, the easy axis is the c axis, [001]. The overall phase diagram of pure MnF_2 is discussed in Ref. 18. Two more recent studies are described in Refs. 19 and 20. The last reference contains the most detailed and most accurate results for the bicritical region. A mean-field treatment of the phase diagram of Zn-doped MnF_2 was given by Brady Moreira *et al.*[21] Because this theory does not include random fields, it is useful as a baseline for assessing the effects of random fields on the experimental data.

This paper is arranged as follows. The experimental techniques are described in Sec. II. The results for the three phase boundaries $H_{sf}(T)$, $T_c^{\parallel}(H)$, and $T_c^{\perp}(H)$ are described and discussed in Secs. III, IV, and V, respectively. A summary of the main results is given in Sec. VI.

II. EXPERIMENTAL

A. Methods of determining phase boundaries

Two different methods for observing the phase transitions were used: dilatometry and measurements of the ultrasonic attenuation. In the first, the length l of the sample along the c axis was measured either as a function of T at constant H (i.e., thermal expansion) or as a function of H at constant T (isothermal magnetostriction). The fractional change in length $\Delta l/l$ is proportional to the derivative $\partial\Psi/\partial p$ of the thermodynamic potential $\Psi(T,H,p)$, where p is a uniaxial pressure along the c axis.[22] Therefore, a first-order transition is accompanied by a discontinuity in l. A second-order transition is accompanied by λ anomalies in the thermal-expansion coefficient $(1/l)(\partial l/\partial T)$ and the differential magnetostriction $(1/l)(\partial l/\partial H)$, which are proportional to second derivatives of Ψ. [As discussed later, we have actually used the derivative $\partial l/\partial(H^2)$ instead of $(\partial l/\partial H)$.] A microscopic treatment of magnetostriction and magnetic thermal expansion (which contains some approximations) was given by Callen and Callen.[23] It relates the variation of l to (1) the variation of those static spin-correlation functions which govern the exchange and anisotropy energies, and (2) the derivatives of the exchange and anisotropy constants with respect to strain.

The second method of observing phase transitions involved measurements of the attenuation of longitudinal sound waves with propagation vector $\vec{q}$ parallel to the c axis. The same ultrasonic technique was used in early investigations of the phase transitions of pure MnF_2 and other antiferromagnets.[18,24] The spin-flop transition at H_{sf} is accompanied by a sharp spike in the attenuation. This spike is believed to be caused by the coexistence of AF and SF domains at the transition.[24,25] The second-order transitions are accompanied by λ peaks in the at-

tenuation. This critical attenuation is reviewed in Ref. 26. In the limit of zero ultrasonic frequency, the maximum attenuation is expected to coincide with the critical temperature T_c. In the present work we used frequencies of 23 and 31 MHz. To our knowledge, in all previous works on (undoped) magnetic materials the attenuation maximum for frequencies in the range 20—30 MHz occurred at a reduced temperature $t=T/T_c$ which differed from unity by less than 1 part in 10^4. (Somewhat larger deviations were reported in some cases for much higher frequencies.[27] These might have been caused by additional attenuation mechanisms in the ordered phase, which caused the attenuation maximum to be shifted to a lower temperature.)

In our previous studies of the phase diagrams of undoped antiferromagnets (e.g., Ref. 28), very good agreement was found between the results obtained from dilatometry and ultrasonic attenuation. However, in the present work small discrepancies between the T_c's obtained from the two methods appeared for those transitions which were broadened by random fields. We shall display both sets of data. However, we regard dilatometry as a more trustworthy method of obtaining T_c because it is a static method which is based on thermodynamics.

B. Samples

A boule of Zn-doped MnF_2 was grown by the Crystal Physics Group, Center for Materials Science and Engineering, Massachusetts Institute of Technology. A Czochralski technique was used. The growth direction was parallel to the a axis. A 2.7-mm-wide plate was obtained from the boule by making two parallel cuts perpendicular to the growth direction. Three samples were then cut from adjacent regions of the plate. Two of these were used in the experiments reported here. The third (which touched the other two before the plate was cut) was used in atomic-absorption analysis. This analysis gave $x=0.125\pm0.013$ where x refers to the formula $Mn_{1-x}Zn_xF_2$.

Several facts indicate that the concentration gradient in the samples was rather small: (1) For a given sample, the concentration gradient led to a rounding of the transition at T_N. The temperature interval over which the transition was rounded was approximately 0.2 K. The corresponding variation of x is $\Delta x\sim3\times10^{-3}$, or $\Delta x/x\sim2\times10^{-2}$. (2) The Néel temperatures for the two samples were both 9 K lower than that in pure MnF_2, but differed from each other by only 0.02 ± 0.05 K. This indicates that the average concentrations in these two samples were very nearly the same, which suggests that the concentration gradient was small. A similar conclusion is reached from a comparison of the spin-flop fields for the two samples at 4.2 K.

The two samples were rectangular parallelepipeds, each with dimensions of $7\times5\times2.7$ mm^3. The long dimension was parallel to the c axis, [001]. The two end faces were lapped parallel to each other. The orientation of these faces was within 0.5° from the crystallographic c face. Detailed measurements were performed only on one of the two samples, which will be labeled as sample 1. The second sample (no. 2) was used only to check several of the results. Some data were also taken on a sample of pure MnF_2 for comparison purposes. Unless otherwise stated, all the results below are for sample 1.

C. Dilatometry

Changes in the length l of the sample were measured with a capacitance dilatometer made of copper. The design was similar to that of the brass dilatometer described earlier.[29] Strictly, the capacitance change corresponded to a change in l relative to that of a copper sample of equal length. However, copper has no thermal-expansion anomalies and its magnetostriction is negligible compared to that of any of our samples.

One difficulty with our capacitance dilatometry is that a spurious signal can develop due to a torque on the sample. Such a torque occurs when the susceptibility is anisotropic and $\vec{H}$ is not parallel to a symmetry axis. For a given misalignment of $\vec{H}$, the torque is largest at $T\ll T_N$ where the anisotropy of the susceptibility is largest. It is much smaller for temperatures near T_N. In the present work the spurious effect caused by the torque was virtually eliminated by carefully aligning $\vec{H}$ parallel to the c axis. A useful sign of the absence of a significant torque is a negligible magnetostriction below the spin-flop transition at 4.2 K. (The magnetoscriction at 4.2 K is discussed later.)

Two types of measurements were made: (1) thermal expansion (TE), i.e., l vs T at constant applied field H_0, and (2) magnetostriction (MS), i.e., l vs H_0 at constant T. In both types of measurements, l was always the length of the sample along the c axis, i.e., $\hat{l}\,||[001]$.

D. Ultrasonic attenuation

Ultrasonic measurements were made with the pulse-echo technique. A single X-cut quartz transducer was used for sending and receiving the longitudinal sound waves. It was bonded to the sample with Nonaq stopcock grease. The propagation vector $\vec{q}$ was parallel to [001]. Changes in the ultrasonic attenuation (UA) were measured by monitoring

the height of a single echo. The results were checked by changing the echo.

The technique of monitoring a single echo is convenient, but is not ideal because the signal is affected by (1) small drifts in the amplitude of the rf pulse used to drive the transducer, (2) small drifts in the amplifiers of the receiver, and (3) small changes, as a function of T, in the coupling between the transducer and the sample. Nevertheless, in nearly all cases the technique gave the locations of the attenuation peaks and their approximate sizes and shapes. The exceptional cases, when the transitions were broad and the signal weak, will be pointed out explicitly.

E. Temperature control and measurement

A system consisting of two concentric copper cans separated by a vacuum space was used. The inner can, which contained the sample and the dilatometer, was filled with helium exchange gas. The entire arrangement was immersed in a liquid-helium bath. A heater, wound on the outer surface for the inner can, worked against a small heat leak from the inner can to the bath. Near 60 K the maximum cooling rate of the sample (when no heat was applied) was ~ 30 mK/min. By adjusting the heat the temperature was either stabilized (to within a few mK when necessary) or made to drift at a nearly constant rate. In the latter case, a cooling rate of ~ 30 mK/min and heating rates of 30–60 mK/min were used.

Temperatures in the range $54 < T < 59$ K (which contained T_N and the bicritical temperature T_b) were measured with a thermistor resistance thermometer attached directly to the sample with G.E. 7031 varnish. The sensitivity was such that a temperature change of 0.7 mK could be detected. The thermistor was calibrated *in situ* and at $H=0$ against a platinum thermometer. The magnetoresistance of the thermistor was proportional to H^2, and at 56 K was equivalent to -30 mK at 100 kOe. A correction for this magnetoresistance was made taking into account its small dependence on T. Data taken at different cooling and heating rates showed the existence of a lag of several mK between the temperatures of the sample and of the thermistor. To determine T_N we averaged the results for comparable heating and cooling rates. For $T_c(H)-T_N$ we used data for T_c and T_N obtained with the same cooling and heating rates. The estimated precision of the thermometry varied from 5 mK at $H=0$ to 15 mK at 140 kOe. The precision in the locations of the transitions was worse because it was also limited by the finite widths of the transitions. The calibration of the reference platinum thermometer had an absolute accuracy of 0.04 K, but this was unimportant for the determination of the H-induced *shifts* of T_c.

All data below 54 K were taken with T held constant to within ~ 0.1 K. Temperatures in the range $25 < T < 54$ K were measured with the platinum thermometer, which was attached to the copper frame of the dilatometer. (The dilatometer was also used in the ultrasonic measurements, but in this case it served merely as a copper block.) The thermometer was read at $H=0$ and also at the transition field. The latter value was corrected for the magnetoresistance.[30] The accuracy of the measured temperatures depended on T; it changed from 0.4 K at 25 K to 0.1 K above 45 K. Measurements at 4.2 K were made by introducing helium exchange gas into the space between the two copper cans.

F. Field alignment

Magnetic fields were produced by a superconducting magnet and by a Bitter magnet. The former generated fields up to 110 kOe and the latter fields up to 140 kOe. In both cases the applied magnetic field H_0 was known to an accuracy of 0.2%.

All data were taken with $\vec{H}_0$ parallel to [001]. The alignment in the superconducting magnet was better than 0.1°, and better than 0.05° in the Bitter magnet. The only exceptions to this statement were some measurements on pure MnF_2 in which the field was aligned to within $\sim 1°$. It is known that the phase boundaries in the bicritical region are particularly sensitive to alignment. It is therefore noteworthy that all the ultrasonic data near the BCP were taken in the Bitter magnets (i.e., alignment better than 0.05°). The dilatometry data near the BCP were taken in both magnets.

The field alignment was accomplished by mechanical devices which controlled the orientation of the sample holder. The alignment was made at the spin-flop transition, which is sensitive to the direction of $\vec{H}$.[31] In the ultrasonic experiments we used the fact that the attenuation peak at H_{sf} is largest for perfect field alignment.[24] To align the sample, this peak was maximized at a fixed temperature between 40 and 45 K. In the dilatometry experiments we assumed that the jump in the sample's length at H_{sf} was sharpest for a perfect field alignment. Possible factors which limited our ability to align the sample were small variations in the direction and magnitude of the demagnetizing field (discussed later) and a mosaic spread in the sample.

G. Demagnetization correction

We shall distinguish between the applied magnetic field $\vec{H}_0$ and the internal magnetic field $\vec{H}$ inside the sample. The two differ by a demagnetizing field

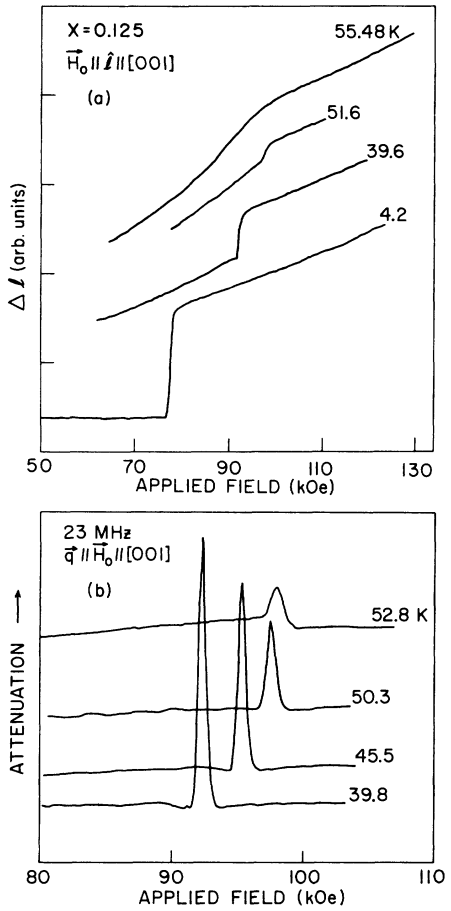

FIG. 1. (a) Traces of the magnetostriction at several temperatures. Δl for $\hat{l} \| [001]$ is the change in the length of the sample along [001]. Lowest three curves show spin-flop transitions. Upper curve shows a P-AF transition near 89 kOe. (b) Examples of the attenuation spike at the spin-flop transition for several temperatures. Traces are for a 23-MHz longitudinal sound wave with a propagation vector $\vec{q} \| [001]$.

$\vec{H}_D$. The latter field is uniform in an ellipsoidal sample, but not in the nonellipsoidal samples used here. Fortunately, $|H_D/H_0|$ was always less than $\sim 0.3\%$, so that a rough estimate of the demagnetization correction was sufficient. For this purpose a demagnetizing factor was estimated from the shape of the sample, and the susceptibility data of pure MnF_2 as a function of T/T_N (Ref. 32) were used. The estimated demagnetization correction for the Zn-doped samples in the temperature range between T_b and T_N was 0.25%. The correction for the spin-flop field varied between 0.1% at 4.2 K and 0.25% near T_b.

Throughout this paper the magnetic field which appears in plots of the raw experimental data is the applied field H_0. However, in plots of the phase diagram the field is always the internal field H.

III. SPIN-FLOP TRANSITIONS

A. Magnetostriction

The spin-flop transition at $H_{sf}(T)$ was accompanied by a jump in the sample's length l. At 4.2 K the magnitude of this jump was $\Delta l/l = (2.3 \pm 0.4) \times 10^{-5}$, which is comparable to that in pure MnF_2.[33] At higher temperatures the jump in l became progressively smaller and was superimposed on a gradual rise of l with increasing H_0. This is illustrated by the lowest three traces in Fig. 1(a). On approaching the bicritical temperature, $T_b = 55$ K, the abrupt jump became very small and it changed gradually into an inflection point on the curve for l vs H_0. This inflection point was quite clear above T_b, and was associated, at these temperatures, with the P-AF transition. An example for $T = 55.48$ $K > T_b$ is shown in Fig. 1(a). The temperature where the jump in l changed into an inflection point (i.e., where the transition changed from first to second order) was not determined precisely. That is, the order of the observed transitions between 54 K and $T_b = 55$ K was uncertain.

At 4.2 K a negligible MS was observed below H_{sf}. This can be understood as follows. The MS is determined by the H dependence of those static spin-correlation functions which govern the exchange and anisotropy energies.[23] For pure MnF_2 at $T = 0$, all static spin-correlation functions are expected to be H independent below H_{sf} so that no MS should be observed below H_{sf}. The situation for pure MnF_2 at 4.2 K is essentially the same, i.e., the MS below H_{sf} should be negligible. In Zn-doped MnF_2 at 4.2 K, the correlation functions for spins which are separated by large distances (compared to a lattice unit) might be affected by H below H_{sf}.[15] However, the exchange energy, and to a large extent also the anisotropy energy,[34] are dominated by the static correlation functions of spins which are separated by distances of less than several lattice units. We expect that these correlation functions are practically H independent below H_{sf} for $x = 0.125$ at $T = 4.2$ K. [One mechanism which can change these correlation functions is the "exchange flip."[35] However, in the present case only one such flip (with $n = 1$ in the notation of Ref. 35) is allowed below H_{sf}, and it involves only a very small percentage of spins.] Thus, we expect a negligible MS below H_{sf} at $T = 4.2$ K. At much higher temperatures the exchange and anisotropy energies depend on H, even below H_{sf}, and a MS is observed.

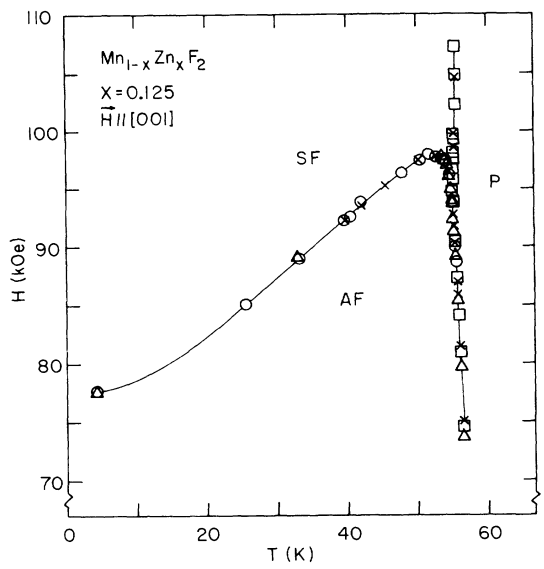

FIG. 2. Spin-flop phase boundary $H_{sf}(T)$, which separates the AF phase from the SF phase. Also shown are portions of the other phase boundaries near the BCP. Data points are circles and triangles from magnetostriction measurements, squares from TE measurements, and crosses from UA measurements. H is the internal magnetic field. Some data points near the BCP were deleted to avoid overcrowding. Lines are merely guides to the eye.

B. Ultrasonic attenuation

The spin-flop transition was accompanied by a sharp spike in the attenuation coefficient Γ as a function of H_0. The spike was at the same field for increasing and decreasing H_0. The magnitude of this spike decreased with increasing T. Examples of experimental results are shown in Fig. 1(b). For the trace at 39.8 K, the magnitude of the spike is ~ 1.2 dB/cm. At temperatures not far below $T_b = 55$ K, the spike was superimposed on a λ anomaly in the attenuation versus H_0. The temperature at which the spike disappeared entirely and only a λ anomaly remained was not determined precisely. Thus, as in the case of the MS data, the order of the transition between 54 K and T_b was unclear.

C. Spin-flop phase boundary

The spin-flop phase boundary H_{sf} vs T is shown in Fig. 2. As can be seen, there is good agreement between the MS results and the ultrasonic data. We shall discuss the results at low T and at high T separately.

1. Low-T value of H_{sf}

At 4.2 K, $H_{sf} = 77.7 \pm 0.2$ kOe for sample 1 and $H_{sf} = 77.8 \pm 0.2$ kOe for sample 2. Both values are $(16 \pm 1)\%$ lower than the corresponding value for pure MnF_2. A mean-field treatment, which ignores random fields and the variation of the lattice constants with doping, predicts that $H_{sf}(T=0)$ scales as $(1-x)$ in the $Mn_{1-x}Zn_xF_2$ system.[21] The measured H_{sf} is approximately 4% lower than this prediction. The lattice constants and the c/a ratio for ZnF_2 are slightly smaller than those for MnF_2. Therefore it is expected that if the variation in the lattice parameters were included in the mean-field treatment, it would have resulted in higher exchange and anisotropy fields, and, hence, in a higher value for H_{sf}. Thus the discrepancy between the observed H_{sf} and the mean-field result is probably slightly larger than 4%.

The deviation from the mean-field result will be attributed to random fields, which by themselves can cause a spin flop.[4] In other words, the field $\vec{H}$ produces a random field $\vec{H}_R$ which leads to an additional tendency of the spins to flop. This lowers H_{sf}. To expand on this idea we shall first review the physics of the spin-flop transition of a ferromagnet in a random field, and then return to the present case of a diluted antiferromagnet in a (real) magnetic field.

Consider a uniaxial ferromagnet in a uniaxial (parallel) random field.[4] Let $T=0$. In the flopped configuration (transverse configuration), each spin adjusts its direction to take advantage of the local parallel random field. Thus the local magnetization also has a longitudinal component which varies randomly from site to site (see Fig. 2 of Galam and Aharony[4]). The free energy of this true flopped configuration is lower than that of an hypothetical flopped configuration with no random field, in which all the spins point along the same (transverse) direction. In the longitudinal phase, with all spins parallel to the easy axis, the spins cannot take advantage of the local random field. Thus, the random field prefers the flopped configuration. This preference is in competition with the anisotropy energy which prefers the longitudinal configuration. For a sufficiently high random field, a spin-flop transition to the flopped configuration takes place.

The situation for a random-site antiferromagnet in a parallel magnetic field and at $T=0$ is similar. For a given sublattice, the orientation of each spin in the flopped phase will depend on the distribution of the nonmagnetic cations (Zn) in its vicinity. This orientation will be determined by the sum of the magnetic field $\vec{H}$, the local exchange field $\vec{H}_E$(local) which acts on the spin, and the local anisotropy field

(which is relatively weak in our system). Thus, there is a distribution of spin orientations for a given sublattice. The free energy of this true flopped configuration is lower than that of the mean-field flopped configuration, in which all the spins on a given sublattice have the same orientation. Thus there is a greater incentive for the spins to flop than that given by the mean-field theory. As a consequence, the spin-flop field H_{sf} is lower. It is noteworthy that in the flopped configuration the local staggered magnetization has a longitudinal component which fluctuates with position. It arises in two ways: (1) Only one of two neighboring cations on opposite sublattices may be magnetic, and (2) even when both cations are magnetic, the parallel component of one spin may be different from that of the other.

To estimate the depression of H_{sf} we relate the present situation to the known problem of the transverse susceptibility $\chi_\perp$ of a diluted antiferromagnet at low H.[36,37] When the anisotropy field H_A is small compared to the exchange field H_E, $\chi_\perp$ is higher than the mean-field value $\chi_\perp^{MF}$. The physical reason is the fluctuation in the orientations of the spins on a given sublattice (for nonzero H), which is very similar to the fluctuation in the SF phase when $\vec{H}$ is along the easy axis. When $H_A/H_E \ll 1$, and for $x \ll 1$, $\chi_\perp$ is larger than $\chi_\perp^{MF}$ by a factor $1+0.784x$.[37] We expect a similar enhancement of the susceptibility χ_{sf} in the SF phase when $\vec{H}$ is parallel to the easy axis. Note that the Gibbs-type free energy $\Psi(T,H)$ contains the terms $-(\frac{1}{2})\chi H^2$ (Ref. 18), so that a higher χ_{sf} implies that the free energy of the flopped configuration is lower than that given by the mean-field theory.

A standard thermodynamic argument relates H_{sf} to the anisotropy energy K at $H=0$, and the difference between χ_{sf} and the parallel susceptibility $\chi_{||}$, namely,[18]

$$H_{sf}=[2K/(\chi_{sf}-\chi_{||})]^{1/2} . \quad (1)$$

In pure MnF_2, $\chi_{||} \ll \chi_{sf}$ at $T=0$. We expect that the same is true for $x=0.125$. Thus, $H_{sf} \propto \chi_{sf}^{-1/2}$ at low T. When $H_A/H_E \ll 1$, χ_{sf} is nearly equal to $\chi_\perp$. The enhancement of χ_{sf} (relative to the mean-field value) should then be approximately the same as that for $\chi_\perp$. Using the calculated $\chi_\perp$ in Ref. 37 for $H_A/H_E \ll 1$ and $x \ll 1$, we estimate that H_{sf} for $x=0.125$ is 4.6% lower than the mean-field value. It we take into account the finite value of H_A/H_E in MnF_2, the estimate changes to 3.6%. These values are comparable to the deviation of the observed H_{sf} from the mean-field prediction.

2. *Behavior near T_b*

An unusual feature of Fig. 2 is the decrease of H_{sf} between 53.5 K and $T_b=55$ K. This is shown more clearly in Fig. 3. A similar behavior was also observed (although less clearly) in a sample with $x=0.04$ (Ref. 13), but not in pure MnF_2.[19,20] The cause of this decrease of H_{sf} is unknown. One possibility is the following. According to Aharony[4] the spin-flop line may split into two second-order lines which surround an intermediate phase between the AF and SF phases. These lines reunite at a higher temperature where they meet the $T_c^{||}$ and $T_c^{\perp}$ lines. This meeting point is then a tetracritical point and not a BCP. As already noted, we were unable to ascertain the order of the transitions on that portion of the spin-flop line for which dH_{sf}/dT was negative. Thus it is possible that these transitions were actually on the higher of the two second-order lines which surround the intermediate phase. The fact that the lower second-order line was not observed does not disprove this conjecture, because the anomalies in the UA and MS at these transitions might have been too weak to be observed or were masked by the stronger anomalies on the nearby upper line.

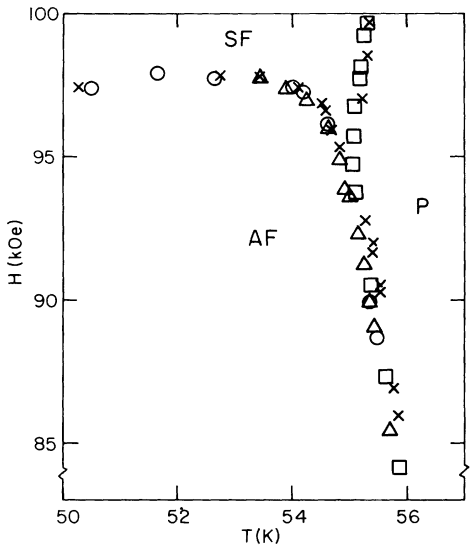

FIG. 3. Expanded view of the high-T portion of Fig. 2. Here, all data points are included.

Another possible cause of the decrease of H_{sf} is the residual misalignment of $\vec{H}$. We believe that this possibility is unlikely because consistent results were obtained in different runs with independent alignments. Also, no such feature was observed in the measurements on pure MnF_2 reported in Ref. 19, in which the alignment was controlled to an accuracy comparable to that in the present experiments.

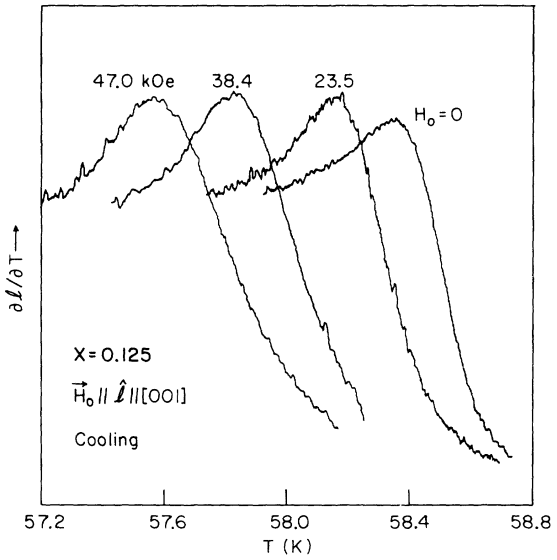

FIG. 4. λ anomalies in the differential TE, $\partial l/\partial T$, for several fixed values of the applied magnetic field H_0. These curves are from data for decreasing T (i.e., cooling).

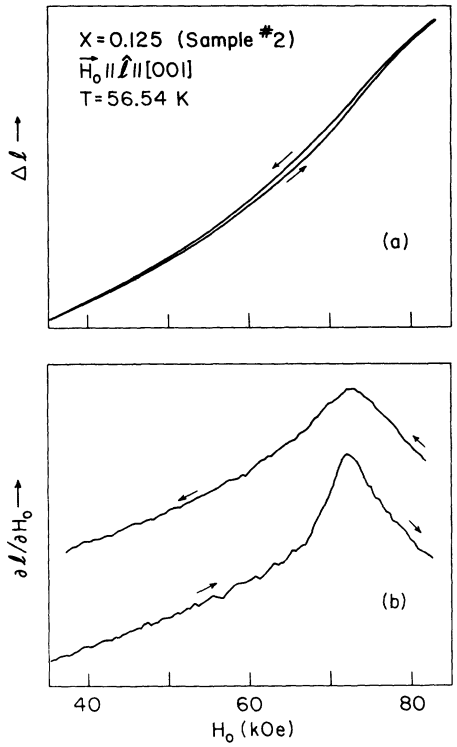

FIG. 5. (a) Magnetostriction at 56.54 K for increasing and decreasing H_0. (b) Differential magnetostriction $\partial l/\partial H_0$ corresponding to (a). The two curves in (b) [but not in (a)] are displaced vertically relative to each other.

IV. P-AF TRANSITIONS

A. λ anomalies

1. Dilatometry

The P-AF transitions were observed in the TE and MS measurements. In the former the transition appeared as an inflection point in the raw data for l vs T at a fixed H_0. This inflection point corresponded to a λ anomaly in the derivative $\partial l/\partial T$. Examples of such λ anomalies, for fairly low fields, are shown in Fig. 4. These curves were obtained by a numerical differentiation of the raw data for l vs T. Note that as H_0 increases, the T variation of $\partial l/\partial T$ on the high-T side of the anomaly becomes more gradual. Thus the anomaly becomes more symmetric with increasing H_0. An increase in the symmetry of the λ peak was observed earlier in heavily doped MnF_2 and FeF_2 (birefringence data)[14] and $FeCl_2$ (specific-heat data).[10]

Two qualitative explanations of the increased symmetry of the λ anomaly with increasing H have been proposed. The first, by Belanger *et al.*,[14] is based on the idea that random fields reduce the effective lattice dimensionality. The second, by Wong *et al.*,[10] focuses on the temperature variation of the magnitude of the random field H_R for a constant H. This variation arises from the T dependence of the susceptibility.

The P-AF transition was also observed in the MS data. It appeared as an inflection point in the raw data for l vs H_0 (or l vs H_0^2) at a fixed T. The inflection point corresponded to a λ anomaly in $\partial l/\partial H_0$ [or $\partial l/\partial(H_0^2)$].

2. Irreversible behavior

An unusual irreversible behavior in the TE and MS data was observed near the P-AF transitions at finite H_0. This is illustrated by the raw MS data in Fig. 5(a) and the corresponding results for $\partial l/\partial H_0$ in Fig. 5(b). These data are for sample 2. The main feature is a small hysteresis in l vs H_0. It corresponds to a larger derivative $\partial l/\partial H_0$ when the transition is approached from the ordered side, i.e., from the low-H side. Also, near the transition the variation of $\partial l/\partial H_0$ in the ordered phase is faster when the transition is approached from the ordered side. The data in Fig. 5 were taken with a sweep rate of 9 kOe/min. A similar behavior was observed in another run with sweep rates between 3 and 15 kOe/min. There was no obvious dependence on the

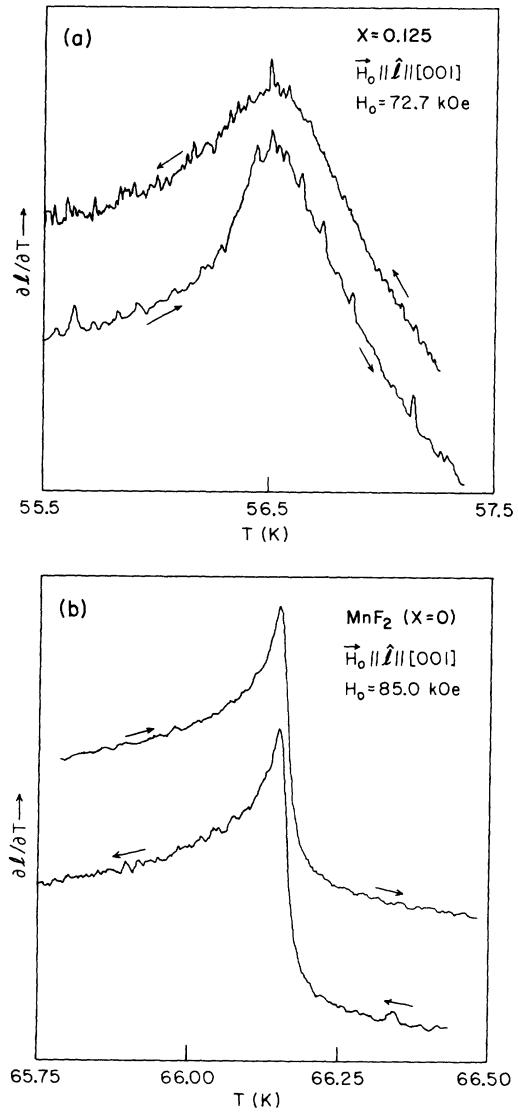

FIG. 6. Differential TE, $\partial l/\partial T$, for increasing and decreasing T. (a) Results for $x=0.125$ at $H_0=72.7$ kOe. (b) Results for pure MnF_2 ($x=0$) at $H_0=85.0$ kOe. In both (a) and (b) the curves for increasing and decreasing T are displaced vertically relative to each other.

sweep rate in this range. An irreversible behavior was also observed in the TE data as illustrated by the results for sample 1 in Fig. 6(a). These data were taken with a sweep rate of approximately 30 mK/min.

The irreversible behavior near the P-AF transition became more pronounced with increasing H_0. At $H_0=0$ there was no detectable irreversibility in $\partial l/\partial T$ near the transition at T_N. Also, no irreversibility in $\partial l/\partial T$ was observed for the transitions on the P-SF boundary $T_c^{\perp}$. These observations suggest that the irreversibility is caused by the random fields which couple to the parallel staggered magnetization.

Because the dilatometry measurements involved the detection of a small mechanical motion of a copper plate (Ref. 29) the possibility that the irreversibility was caused by some sort of a backlash was considered. The evidence against this explanation is the following: (1) As noted, there was no irreversibility in $\partial l/\partial T$ at the Néel point or at the P-SF transitions. (2) A consistent irreversible behavior was observed in four different sets of runs—two for sample 1 and two for sample 2. Each sample was remounted in the dilatometer before each set. (3) A control experiment was performed with the same dilatometer on a sample of pure MnF_2. The TE coefficient was measured near the P-AF transition at high H_0. The sweep rate was comparable to that used with the doped sample (~ 30 mK/min). The results, shown in Fig. 6(b), exhibit no irreversibility. A comparison between Figs. 6(a) and 6(b) also illustrates the sharpness of the transition in pure MnF_2 as compared to that for $x=0.125$.

The evidence presented above suggests that the irreversibility in the TE and MS data is not an experimental artifact. However, it must be mentioned that no obvious irreversibility was observed in the ultrasonic data. Finally, we note that the possibility of irreversibility is not excluded theoretically if $d_l=3$, because then the transition is not a genuine second-order transition.

3. *Ultrasonic attenuation*

Attenuation measurements were made with 23- and 31-MHz longitudinal waves propagating along [001]. λ anomalies in the attenuation coefficient Γ were observed both in measurements of Γ vs T at a fixed H_0 and in measurements of Γ vs H_0 at a fixed T. The two types of data are illustrated by the examples in Fig. 7. In Fig. 7(a) the magnitude of the attenuation peak at $H_0=0$ is ~ 1 dB/cm. No obvious irreversibility was observed in the ultrasonic data.

The data in Fig. 7(a) show the following qualitative features. With increasing H_0 the attenuation peak becomes smaller, more symmetric, and broader. In pure MnF_2 the height of the attenuation peak at $T_c^{\parallel}$ is approximately the same for all H and the peak remains very asymmetric even at high H.[18] Thus, the marked differences in the heights and shapes of the attenuation peaks in Fig. 7(a) are probably caused by the change in the magnitude of the random field. The qualitative features of Fig. 7(a) are similar to those exhibited by the specific-heat

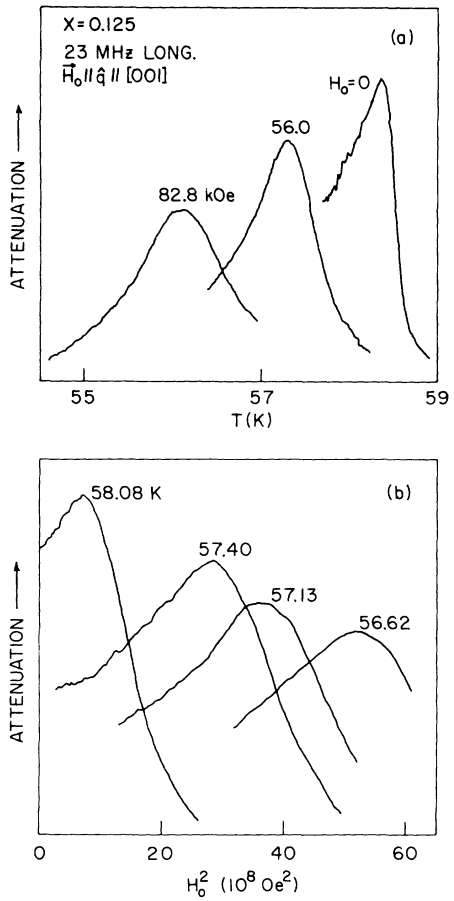

FIG. 7. (a) Traces of the UA vs T for several fixed values of H_0. (b) Traces of the UA vs H_0^2, for several fixed temperatures.

curves for Mg-doped $FeCl_2$.[10]

Two previously proposed explanations for the increased symmetry of the λ anomaly with increasing H were already mentioned in Sec. IV A 1. An explanation of the increased rounding of the transition at high H was also proposed by Belanger *et al.*[14] It is based on the theoretical work of Binder *et al.*[6] for the Ising model in a random field. In the latter work, $d_l=3$ and the "transition" for $d=3$ is smeared. Close to the transition the correlation length ξ is limited by the domain size L_0, which leads to a rounded transition. The rounding increases rapidly with increasing H_R, i.e., with increasing H in the present case.

B. Phase boundary

1. Criterion for $T_c^{\|}$

The rounding of the transition at $T_c^{\|}(H)$ was much larger than that in pure MnF_2. At $H=0$ the rounding was probably caused by a variation of the Zn concentration x inside the sample. The increased rounding with increasing H is believed to be the result of the random fields. The rounding of the transition led to an imprecision in the determination of $T_c^{\|}$. Our choice for the transition temperature (or field) was always the location of the maximum of the λ anomaly. This choice is not rigorously correct, as illustrated by the following example. Assume that x has a symmetric distribution about a mean value $\bar{x}$. Assume further that the λ peak for a given x is asymmetric, which is the case here. Then the temperature T_{max} at the maximum of the λ anomaly (integrated over all x) does not coincide with $T_c(\bar{x})$.[38] In the present case the situation is complicated further by the H dependences of the shape of the λ anomaly and its rounding. Thus the practical choice of T_{max} as T_c leads to a slight error which may be H dependent. This source of error will be discussed later when it is deemed to be significant.

In the ultrasonic experiments the λ anomaly is observed directly, and the location of its maximum is obtained from the raw data. This is not the case in the dilatometry measurements in which l is measured as a function of T or H_0. The λ anomaly is then in derivatives which are obtained from the raw data. When the raw data are for l vs H_0, λ anomalies are observed in derivatives such as $\partial l/\partial H_0$ and $\partial l/\partial(H_0^2)$. If the transition is sharp then the maxima of these derivatives occur at the same H_0. However, for a rounded transition the maxima of $\partial l/\partial H_0$ and $\partial l/\partial(H_0^2)$ are not located at precisely the same H_0. In the present experiments the difference in the locations of these two maxima was rather small. Nevertheless, for consistency, the maximum of $\partial l/\partial(H_0^2)$ was always used as the criterion for $T_c^{\|}$. This choice was motivated by scaling theories for both pure[17] and doped[8] antiferromagnets which suggest that H^2 is the natural variable. In the analysis of the TE data we always used the λ anomaly in $\partial l/\partial T$.

2. Néel temperature

The TE data gave $T_N=58.358\pm0.015$ K for sample 1 and 58.38 ± 0.03 K for sample 2. These numbers represent averages over several experimental runs. The quoted uncertainties do not include the 0.04-K uncertainty in the calibration of the reference platinum thermometer. The UA data for sample 1 gave $T_N=58.356\pm0.01$ K.

According to mean-field theory,[21] T_N in the $Mn_{1-x}Zn_xF_2$ system should scale as $(1-x)$. The measured values for $T_N(x=0.125)$ are 13.3% lower

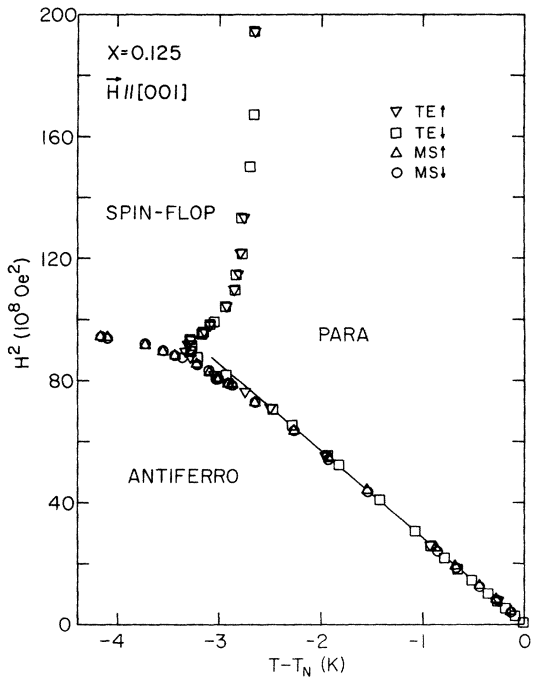

FIG. 8. Phase diagram for the temperature range $T_b \lesssim T \leq T_N$, where T_b and T_N are the bicritical and Néel temperatures, respectively. Results are from dilatometry only. TE↑ and TE↓ are results from TE in increasing and decreasing T, respectively. MS↑ and MS↓ are results from magnetostriction in increasing and decreasing H, respectively. Solid line is a straight-line fit to the low-H data.

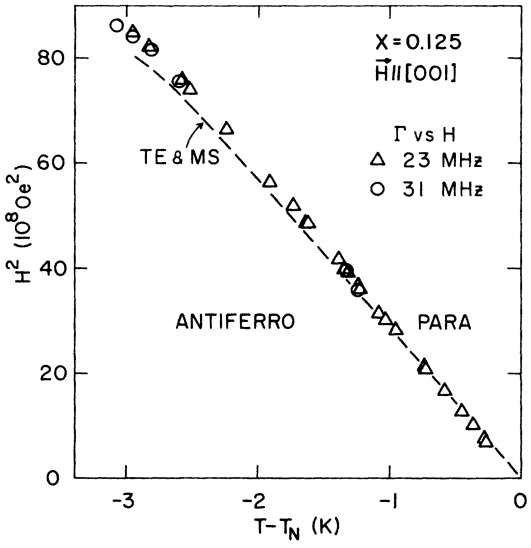

FIG. 9. P-AF phase boundary $T_c^{\parallel}(H^2)$ from traces of the UA Γ vs H. Dashed line is the smoothed phase boundary obtained from dilatometry, i.e., from TE and MS data.

than $T_N(x=0)$, in reasonable agreement with this prediction. A similar result was obtained earlier for $x=0.04$.[13] Our values for T_N are also consistent with the results of Belanger *et al.*[39] and of Salamati-Mashhad *et al.*[40]

3. *P-AF phase boundary*

As noted above, the λ anomalies obtained from the dilatometry data showed some irreversibility near the P-AF transitions at finite H. We shall therefore plot the results for increasing (↑) and decreasing (↓) T or H separately. (This was not done in Figs. 2 and 3, which show averages of $T_c^{\parallel}$ for ↑ and ↓.) Because no obvious irreversibility was observed in the UA data, only averages for ↑ and ↓ will be plotted.

The dilatometry results (from TE and MS) for the P-AF boundary are shown in Fig. 8. The ordinate is H^2. The low-H data points lie on a straight line with $dT_c^{\parallel}/d(H^2) = -3.5\times10^{-10}$ K/Oe^2. Approaching the BCP, the boundary deviates from this straight line in the downward direction.

The determination of the boundary $T_c^{\parallel}(H)$ from data for Γ vs T (with fixed H_0) was only partially successful. At zero and low H_0 the results for $T_c^{\parallel}$ were in good agreement with the dilatometry data. However, above $\sim$50 kOe an increasing scatter in the results for $T_c^{\parallel}$ appeared. This was probably caused by small drifts in the electronics during the time it took to scan the broad attenuation peak (see Sec. II D). In spite of the scatter, it appeared that above $\sim$50 kOe the T_c's obtained from Γ vs T were somewhat higher than those obtained from dilatometry.

Results with a smaller scatter were obtained from scans of Γ vs H_0 at a fixed T. Such scans could be made rather quickly (several minutes per scan). Several scans of the attenuation peak were taken at each T and the values for the transition field were averaged. The results for the boundary $T_c^{\parallel}$ are shown in Fig. 9. (For T_N we used the consistent result obtained from Γ vs T, because T_N could not be obtained from Γ vs H_0.) For comparison, the smoothed phase boundary obtained from the dilatometry data is also shown in Fig. 9. There is good agreement at low H, but a systematic difference of $\sim$0.1 K is found at high H where the λ anomalies are broader. As mentioned, we consider the dilatometry method to be more reliable, in principle, than the ultrasonic method. However, even with this technique the choice $T_{\max} = T_c$ is inexact.

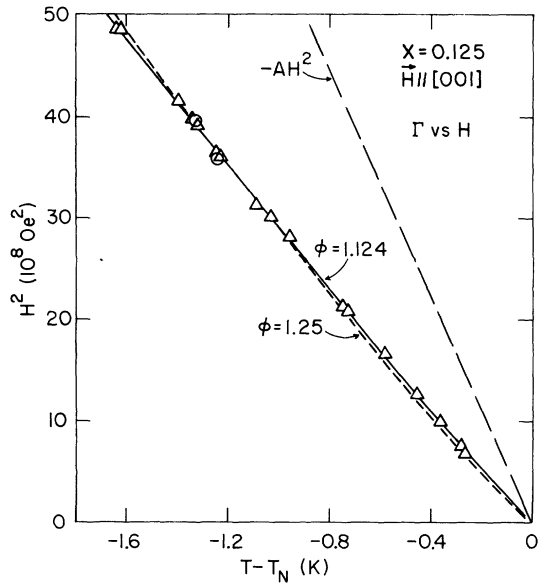

FIG. 10. Expanded view of the low-H results in Fig. 9. Solid line ($\phi=1.124$) is a best fit to Eq. (2) with B and ϕ treated as adjustable parameters and A held fixed at the mean-field value 1.79×10^{-10} K/Oe^2. Short-dashed curve is a best fit with ϕ held fixed at the theoretical value 1.25, A fixed as above, and B treated as an adjustable parameter. Long-dashed straight line is the mean-field prediction with no random fields.

4. *Depression of $T_c^{\|}$ by random fields*

In pure MnF_2, $T_c^{\|}$ decreases linearly with H^2 at low H, with $dT_c^{\|}/d(H^2)\cong-1.57\times10^{-10}$ K/Oe^2 (Ref. 19). A mean-field treatment which ignores random fields[21] predicts that in Zn-doped MnF_2, $dT_c^{\|}/d(H^2)$ will be larger by a factor $(1-x)^{-1}$. That is, $dT_c^{\|}/d(H^2)\cong-1.79\times10^{-10}$ K/Oe^2 for the present case. The measured depression of $T_c^{\|}$ at low H is approximately a factor of two larger than this prediction. This is illustrated by Fig. 10, in which the line $-AH^2$ represents the mean-field prediction. An obvious interpretation is that the additional depression of $T_c^{\|}$ is caused by random fields. A similar additional depression of $T_c^{\|}$ was observed in the $x=0.04$ sample,[13] and more dramatically in more heavily doped samples of MnF_2, FeF_2, and $FeCl_2$.[14,10]

5. *Behavior at low H*

According to Fishman and Aharony[8] the shape of the phase boundary $T_c^{\|}$ at low H should be given by

$$T_c^{\|}-T_N=-AH^2-BH^{2/\phi}\,, \tag{2}$$

where $\phi=1.25$ for $d=3$. The term $-AH^2$ is similar to that in a pure antiferromagnet. The additional term $-BH^{2/\phi}$ is due to the random field H_R which is proportional to H near T_N. Clearly, the latter term produces a curvature in the phase boundary $T_c^{\|}$ vs H^2.

We have compared the results for $T_c^{\|}(H^2)$ in the range $0\lesssim H^2\lesssim5\times10^9$ Oe^2 with Eq. (2). The parameter A was fixed at the value 1.79×10^{-10} K/Oe^2, as estimated earlier. The data of Fig. 8 (from dilatometry) then gave $\phi=1.01\pm0.02$, corresponding to the fact that the phase boundary in this field range is very nearly a straight line. The phase boundary obtained from Γ vs H (Fig. 10) does have a slight curvature, but the least-squares fit gives $\phi=1.12\pm0.02$ which is still well below the predicted value. Thus, no evidence that ϕ is as large as 1.25 is found in our data.

Two recent experiments on more heavily doped antiferromagnets have demonstrated the existence of the term $-BH^{2/\phi}$ with $\phi>1$. The first, by Belanger *et al.*,[14] gave $\phi=1.4$. The second, by Wong *et al.*,[10] gave $\phi=1.25$. In both of these works the term $-BH^{2/\phi}$ was much larger than $-AH^2$ because of the high doping level x. Thus, a better determination of ϕ could be made than in the present work where $-AH^2$ accounted for $\sim50\%$ of the shift in $T_c^{\|}$. Nevertheless, there is still a discrepancy between our values for ϕ and 1.25 which remains to be explained. Two possible sources of error are the following. (i) The choice $T_{\max}=T_c$ which was used was inexact. It probably led to a small error in the shape of the boundary $T_c^{\|}(H)$. As Fig. 10 illustrates, the difference between the results for $T_c^{\|}$ and the fit with the theoretical value $\phi=1.25$ is rather small. Such a difference could have been caused by the choice $T_{\max}=T_c$. (It is noteworthy that Belanger *et al.* used two different criteria for $T_c^{\|}$: one at $H=0$ and another at $H\neq0$. This led to a higher value for ϕ than that which would have been obtained with the choice $T_{\max}=T_c^{\|}$ for all H.) (ii) Equation (2) is valid only very near T_N. Our analysis included shifts of up to 1.7 K in $T_c^{\|}$. Among the reasons why Eq. (2) may not be exact for such large shifts are (a) H_R is not strictly proportional to H over this temperature range,[10] and (b) for the highest fields ($H^2\cong5\times10^9$ Oe^2) the phase boundary may be influenced by the BCP, which tends to produce a curvature opposite to that produced by $-BH^{2/\phi}$. In principle, the analysis could have been limited to much lower H^2, but then the experimental uncertainties would have been more of a problem. In conclusion, although we find no evidence that ϕ is as large as 1.25, the uncertainties in the analysis are such that this value cannot be excluded.

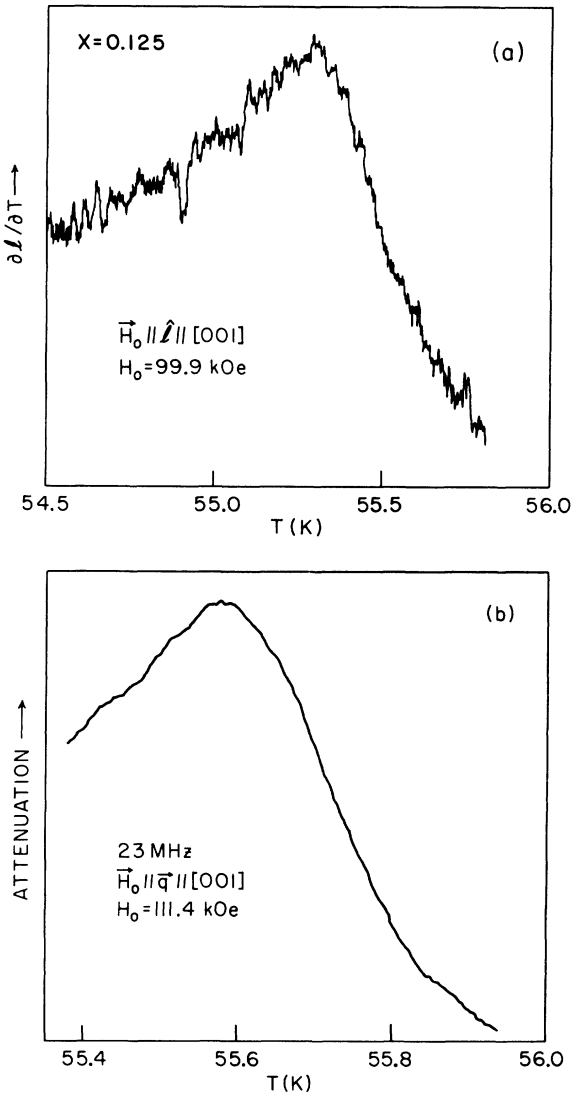

FIG. 11. (a) λ anomaly in the differential thermal expansion $\partial l/\partial T$ at a P-SF transition. (b) λ anomaly in the UA at a P-SF transition.

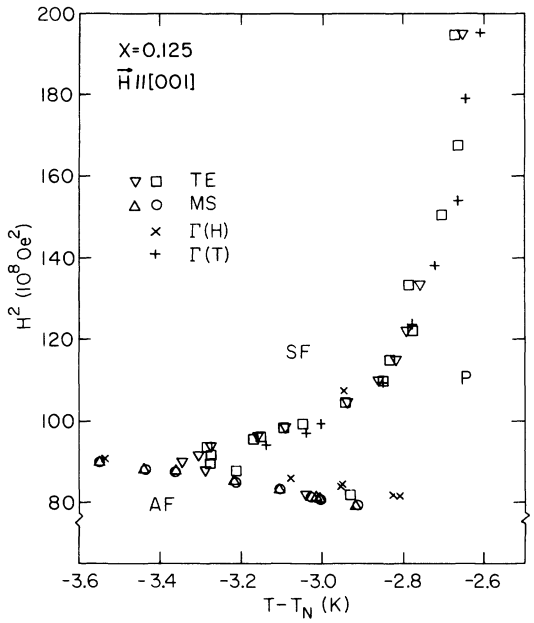

FIG. 12. P-SF phase boundary $T_c^{\perp}$. Also shown are portions of the P-AF boundary and the spin-flop line. Data are from TE and MS measurements (symbols as in Fig. 8) and from the UA (Γ vs H or Γ vs T).

V. P-SF TRANSITIONS

A. λ anomalies

The P-SF transition was readily observed in the TE measurements, in which it appeared as a λ anomaly in $\partial l/\partial T$. An example is shown in Fig. 11(a). In the MS measurements the anomaly in $\partial l/\partial H_0$ did not stand out clearly. This is attributed to the fact that the boundary $T_c^{\perp}(H)$ is very steep.

Transitions on the $T_c^{\perp}$ boundary were also observed in the UA, Γ vs T, as illustrated in Fig. 11(b). Less successful were the measurements of Γ vs H_0. In these the transition was observed only in a limited temperature range near 55.4 K ($T-T_N \cong -3.0$ K). Even in this range the λ peak was small and was superimposed on a larger λ peak from the nearby P-AF transition.

B. Phase boundary

The phase boundary $T_c^{\perp}(H)$ was determined from the locations of the maxima of the λ anomalies. Figure 8 shows this boundary in relation to the other phase boundaries. These data are from dilatometry only. A more detailed plot of the P-SF boundary, which includes also the ultrasonic results, is shown in Fig. 12.

The scatter of the results in Figs. 8 and 12, and the uncertainty in the direction of the spin-flop line at the BCP, prevented a meaningful analysis of the bicritical region in terms of shift exponents and scaling axes.[12,13]

There is a considerable difference between the $T_c^{\perp}$ boundary for $x=0.125$ and that for $x=0$. In both cases $T_c^{\perp}$ increases with H just above the BCP so that the boundary has a "bulge" which points towards high T. However, for $x=0.125$ the magnitude of the bulge is at least 0.6 K, whereas for pure

MnF_2 it is an order of magnitude smaller.[19] This result is consistent with earlier observations in more lightly doped samples of $GdAlO_3$ and MnF_2.[12,13]

VI. SUMMARY

The main results of the present work are as follows:

(i) The random field H_R changes the shape of the λ anomaly at $T_c^{\parallel}$. This is most clearly seen in data for Γ vs T. There, the λ peak becomes smaller, broader, and more symmetric, as H (or H_R) increases. The increased broadening is mainly on the high-T side of the peak. This broadening on the high-T side of the peak is also observed in the results for $\partial l/\partial T$. Similar effects have been observed in earlier studies on other materials.[10,13,14]

(ii) Some evidence for an irreversible behavior near $T_c^{\parallel}$ is found in the dilatometry data for $H \neq 0$. Such a behavior has not been reported previously.

(iii) The random field produces a substantial decrease in $T_c^{\parallel}$, as observed in earlier studies.[10,12–14] A definitive test of the prediction that this decrease is proportional to $H^{2/\phi}$, with $\phi = 1.25$, was not possible.

(iv) The Néel temperature $T_N(x = 0.125)$ is in reasonable agreement with mean-field theory.

(v) The spin-flop field at 4.2 K is lower than that predicted by mean-field theory. The discrepancy is explained by including the effect of random fields. This change of H_{sf} due to the random field has not been discussed previously.

(vi) The spin-flop line $H_{sf}(T)$ bends downwards as T approaches T_b. A similar (but less pronounced) behavior was observed in only one previous study.[13] It is possible that a portion of the apparent spin-flop line near T_b is actually one of two critical lines which surround an intermediate phase.

(vii) The boundary $T_c^{\perp}(H)$ exhibits a much larger bulge (toward high T) than that in pure MnF_2. This result is consistent with earlier observations.[12,13]

ACKNOWLEDGMENTS

The Francis Bitter National Magnet Laboratory is supported by the National Science Foundation. The Institute of Physics at Universidade de São Paulo is supported by Financiadora de Estudos e Projetos (FINEP). This work was supported in part by a joint grant from the U.S. National Science Foundation and the Brazilian Conselho Nacional de Desenvolvimento Científico e Tecnológico (CNPq). We are grateful to S. Foner for editorial comments.

[1] Y. Imry and S.-k. Ma, Phys. Rev. Lett. 35, 1399 (1975).
[2] G. Grinstein, Phys. Rev. Lett. 37, 944 (1976).
[3] A. Aharony, Y. Imry, and S.-k. Ma, Phys. Rev. Lett. 37, 1364 (1976); A. P. Young, J. Phys. C 10, L257 (1977).
[4] See, for example, A. Aharony, Phys. Rev. B 18, 3328 (1978); S. Galam and A. Aharony, J. Phys. C 13, 1065 (1980).
[5] E. Pytte, Y. Imry, and D. Mukamel, Phys. Rev. Lett. 46, 1173 (1981).
[6] K. Binder, Y. Imry, and E. Pytte, Phys. Rev. B 24, 6736 (1981).
[7] G. Grinstein and S.-k. Ma, Phys. Rev. Lett. 49, 685 (1982).
[8] S. Fishman and A. Aharony, J. Phys. C 12, L729 (1979).
[9] A. J. Bray, Phys. Lett. 74A, 129 (1979); J. Phys. C 13, 2361 (1980). See also Ref. 4.
[10] P. Wong, S. von Molnar, and P. Dimon, J. Appl. Phys. 53, 7954 (1982), and unpublished.
[11] D. Mukamel and G. Grinstein, Phys. Rev. B 25, 381 (1982). See also P. Wong, P. M. Horn, R. J. Birgeneau, C. R. Safinya, and G. Shirane, Phys. Rev. Lett. 45, 1974 (1980).
[12] H. Rohrer, A. Aharony, and S. Fishman, J. Magn. Magn. Mater. 15-18, 396 (1980); H. Rohrer and H. J. Scheel, Phys. Rev. Lett. 44, 876 (1980); H. Rohrer, J. Appl. Phys. 52, 1708 (1981).
[13] Y. Shapira, J. Appl. Phys. 53, 1931 (1982).
[14] D. P. Belanger, A. R. King, and V. Jaccarino, Phys. Rev. Lett. 48, 1050 (1982); J. Appl. Phys. 53, 2702 (1982).
[15] H. Yoshizawa, R. A. Cowley, G. Shirane, R. J. Birgeneau, H. J. Guggenheim, and H. Ikeda, Phys. Rev. Lett. 48, 438 (1982).
[16] J. M. Kosterlitz, D. R. Nelson, and M. E. Fisher, Phys. Rev. B 13, 412 (1976).
[17] M. E. Fisher, Phys. Rev. Lett. 34, 1634 (1975).
[18] Y. Shapira and S. Foner, Phys. Rev. B 1, 3083 (1970).
[19] Y. Shapira and C. C. Becerra, Phys. Lett. 57A, 483 (1976); 58, 493(E) (1976).
[20] A. R. King and H. Rohrer, Phys. Rev. B 19, 5864 (1979).
[21] F. G. Brady Moreira, I. P. Fittipaldi, S. M. Rezende, R. A. Tahir-Kheli, and B. Zeks, Phys. Status Solidi B 80, 385 (1977).
[22] W. J. Carr, Jr., in *Handbuch der Physik,* edited by S. Flügge (Springer, Berlin, 1966), Vol. XVIII/2.
[23] E. Callen and H. B. Callen, Phys. Rev. 139, A455 (1965); E. Callen, J. Appl. Phys. 39, 519 (1968). See also Y. Shapira, Donald R. Nelson, and R. D. Yacovitch, Phys. Lett. 53A, 19 (1975); Y. Shapira and R. D. Yacovitch, in *Magnetism and Magnetic Materials—1975 (Philadelphia),* Proceedings of the 21st Conference

on Magnetism and Magnetic Materials, Philadelphia, 1975, edited by J. J. Becker, G. H. Lander, and J. J. Rhyne (AIP, New York, 1976), p. 435.

[24]Y. Shapira, J. Appl. Phys. 42, 1588 (1971); Y. Shapira and J. Zak, Phys. Rev. 170, 503 (1968); Y. Shapira and C. C. Becerra, Phys. Rev. B 16, 4920 (1977).

[25]V. G. Bar'yakhtar and B. A. Ivanov, Zh. Eksp. Teor. Fiz. 66, 1844 (1974) [Sov. Phys.—JETP 39, 907 (1974)]; A. I. Mitsek, N. P. Kolmakova, and D. I. Sirota, Phys. Status Solidi B 72, 807 (1975).

[26]B. Lüthi, T. J. Moran, and R. J. Pollina, J. Phys. Chem. Solids 31, 1741 (1970).

[27]T. J. Moran and B. Lüthi, Phys. Rev. B 4, 122 (1971); A. Bachellerie and Ch. Frenois, J. Phys. (Paris) 35, 437 (1974).

[28]Y. Shapira and C. C. Becerra, Phys. Rev. Lett. 38, 358 (1977); Y. Shapira and N. F. Oliveira, Jr., Phys. Rev. B 17, 4432 (1978).

[29]Y. Shapira and N. F. Oliveira, Jr., Phys. Rev. B 18, 1425 (1978). See also G. K. White, Cryogenics 1, 151 (1961).

[30]L. J. Neuringer, A. J. Perlman, L. G. Rubin, and Y. Shapira, Rev. Sci. Instrum. 42, 9 (1971).

[31]G. K. Chepurnykh, Fiz. Tverd. Tela (Leningrad) 10, 1917 (1968) [Sov. Phys.—Solid State 10, 1517 (1968)]; H. Rohrer and H. Thomas, J. Appl. Phys. 40, 1025 (1969).

[32]C. Trapp, Ph.D. thesis, University of Chicago, 1963 (unpublished); S. Foner, in *Magnetism,* edited by G. T. Rado and H. Suhl (Academic, New York, 1963), Vol. I. p. 383.

[33]K. L Dudko, V. V. Eremenko, and V. M. Fridman, Fiz. Tverd. Tela (Leningrad) 12, 83 (1970) [Soviet Phys.—Solid State 12, 65 (1970)].

[34]F. Keffer, Phys. Rev. 87, 608 (1952).

[35]A. R. King, V. Jaccarino, T. Sakakibara, M. Motokawa, and M. Date, Phys. Rev. Lett. 47, 117 (1981).

[36]A. Brooks Harris and S. Kirkpatrick, Phys. Rev. B 16, 542 (1977).

[37]A. R. King and V. Jaccarino, J. Appl. Phys. 52, 1785 (1981).

[38]J. J. White, H. I. Song, J. E. Rives, and D. P. Landau, Phys. Rev. B 4, 4605 (1971).

[39]D. P. Belanger, F. Borsa, A. R. King, and V. Jaccarino, J. Magn. Magn. Mater. 15-18, 807 (1980).

[40]H. Salamati-Mashhad, G. S. Dixon, and J. J. Martin, J. Appl. Phys. 53, 1929 (1982).